Published in final edited form as:
Oncogene. 2013 November 7; 32(45): 5302–5314. doi:10.1038/onc.2012.624.

Role for Prdx1 as a specific sensor in redox-regulated senescence in breast cancer

Brittany Turner-Ivey[1], **Yefim Manevich**[2], **Jennifer Schulte**[2], **Emily Kistner-Griffin**[3], **Agnieszka Jezierska-Drutel**[2], **Yusen Liu**[4], and **Carola A. Neumann**[5,#]

[1]Department of Pathology, Medical University of South Carolina, Charleston, SC, 29425

[2]Department of Cell and Molecular Pharmacology and Experimental Therapeutics Medical, Medical University of South Carolina, Charleston, SC, 29425

[3]Department of Biostatistics and Epidemiology, Medical University of South Carolina, Charleston, SC, 29425

[4]The Research Institute at Nationwide Children's Hospital, Columbus, OH 43205.

[5]Department of Pharmacology and Chemical Biology, University of Pittsburgh, Pittsburgh, PA, 15213 Magee-Womens Research Center, UPCI, Pittsburgh, PA15213

Abstract

Recent studies suggest that Peroxiredoxin 1 (Prdx1), in addition to its known H_2O_2-scavenging function, mediates cell signaling through redox-specific protein-protein interactions. Our data illustrate how Prdx1 specifically coordinates p38MAPK-induced signaling through regulating p38MAPKα phosphatases in a H_2O_2-dose dependent manner. MAPK phosphatases (MKP-1 and/or MKP-5), which are known to dephosphorylate and deactivate the senescence-inducing MAPK p38α, belong to a group of redox-sensitive phosphatases (protein tyrosine phosphatases: PTPs) characterized by a low pKa cysteine in their active sites. We found that Prdx1 bound to both MKP-1 and MKP-5, but dissociated from MKP-1 when the Prdx1 peroxidatic cysteine Cys52 was over-oxidized to sulfonic acid, which in turn resulted in MKP-1 oxidation-induced oligomerization and inactivity towards p38MAPKα. Conversely, over-oxidation of Prdx1-Cys-52 was enhancing in the Prdx1:MKP-5 complex with increasing amounts of H_2O_2 concentrations and correlated with a protection from oxidation-induced oligomerization and inactivation of MKP-5 so that activation towards p38MAPK was maintained. Further examination of this Prdx1-specific mechanism in a model of ROS-induced senescence of human breast epithelial cells revealed the specific activation of MKP-5, resulting in decreased p38MAPKα activity. Taken together, our data suggest that Prdx1 orchestrates redox-signaling in a H_2O_2-dose dependent manner through the oxidation-status of its peroxidatic cysteine Cys52.

Introduction

A role for reactive oxygen species (ROS) in cell signaling has long been accepted, however, detailed evidence demonstrating their specific impact on signaling events is still lacking. Recent studies from our laboratory and others suggest that one possible mechanism is via protein oxidation, thereby modifying protein function. Cellular ROS impacts signaling through their localized accumulation, if we consider ROS as byproducts of the electron transport chain in the mitochondria or activation of NADPH oxidases. This requires the local and timely availability of ROS-scavenging enzymes at the time of ROS build up, in

[#]Corresponding author Voice: 412 641 7725 Fax: 412 641 2458 neumannc@upmc.edu.

order to protect proteins from oxidation-induced modifications affecting cell signaling. A new class of peroxidases,the peroxiredoxins (Prdxs), offer such flexibility since they are not as compartimentalized in the cell as catalase. Prdxs (Prdx1-6) are a superfamily of small nonseleno peroxidases (22-27 kDa) currently known to comprise six mammalian isoforms. Prdxs 1-5 are classified as 2-Cys Prdxs and Prdx6 as 1-Cys Prdx (1). In typical 2-Cys Prdxs, like the mammalian Prdx1, the peroxidatic cysteine (Cys52 in Prdx1) reduces H_2O_2 to H_2O and becomes oxidized to sulfenic acid. The resolving cysteine (Cys173 in Prdx1) of another subunit reacts with the sulfenic acid to form an intramolecular disulfide, which can be reduced by thioredoxin (Trx). Thioredoxin is then reduced by NADPH-dependent thioredoxin reductase. Over-oxidation of Prdx1's Cys52 renders the peroxidase inactive (2-4). Recent evidence suggests Prdx1 may be a “fine tuner” of cellular H_2O_2-signaling by regulating the activity of binding partners (4) such as JNK (5), c-Abl kinase (6) and as we have recently shown, the phosphatase PTEN (7).

We demonstrate that Prdx1 regulates p38MAPKα activity in senescence signaling by differentially modulating the activity of two p38MAPKα phosphatases, MAP kinase phosphatase 1 (MKP-1) and MKP-5. P38MAPKα, an essential mediator of senescence (8), is activated by several different MAPK kinases (MAP2K). Among these, ASK1 (apoptosis signal-regulating kinase 1) and MAPK kinases (MKKs), such as MKK3, MKK4, and MKK6, mediate ROS-induced senescence by activating p38MAPK-α through phosphorylation on Thr180 and Tyr182 (9). P38MAPKα is dephosphorylated and inactivated predominantly by MKP-1 and MKP-5(10) . Like PTEN, MKPs belong to the class of protein tyrosine phosphatases characterized by a catalytic low pK_a cysteine residue (pK_a 4.7-5.4) located within a conserved motif of its active site, which when oxidized abolishes its nucleophilic properties. This process renders the phosphatase inactive (11, 12), leading to disulfide-based oligomeric structures reducible by β-ME (13). We’ve shown that Prdx1 binding to PTEN is essential for the protection of PTEN lipid phosphatase activity from oxidation-induced inactivation in oncogenic Akt signaling (7), suggesting a role for Prdx1 in regulating oxidation-sensitive phosphatases. In our present study, we are e extending the role for Prdx1 as a specific regulator of redox signaling. While Prdx1 bound to both MKP-1 and MKP-5, it only dissociated from MKP-1 under H_2O_2-induced stress, thereby allowing H_2O_2-induced oligomerization of MKP-1 and loss of its activity towards p38MAPKα. Prdx1 protected MKP-5 from oxidation-induced inactivation at high concentrations of H_2O_2, promoting MKP-5 activity towards p38MAPKα. Unexpectedly, binding of Prdx1 to MKP-1 and MKP-5 seemed regulated by over-oxidation of Prdx1's peroxidatic cysteine Cys52: while Prdx1-Cys52-SO3 did not bind to MKP-1, it was enhanced with MKP-5 under increasing oxidative stress. This redox-specific regulation was especially relevant in p38MAPKα-mediated senescence in human malignant breast epithelial cells (MCF-7), where Prdx1 only promoted the activity of MKP-5, thereby preventing p38MAPKα-mediated senescence.

Results

Lack of Prdx1 promotes senescence and p38 MAPK activation in murine fibroblasts

Murine embryonic fibroblast (MEFs) isolated from *Prdx1*$^{-/-}$ embryos (14) undergoing the 3T3 protocol (15) did not gain exponential growth in the first several months compared to *Prdx1*$^{+/+}$MEFs (Fig.S1). In addition, plotting cell number versus passage number showed that *Prdx1*$^{-/-}$MEFs enter senescence and crisis at passage 5-7, whereas *Prdx1*$^{+/+}$MEFs divided more frequently before entering senescence at passages 12-15 (Fig.1A). We therefore sought to investigate if Prdx1 regulates cellular senescence. First, we analyzed MEFs undergoing processes of spontaneous immortalization induced by passaging for signs of senescence. *Prdx1*$^{-/-}$MEFs rapidly manifested a senescent morphology and exhibited

positive blue staining for senescence-associated β-galactosidase (SA-βgal$^+$) activity. At passages 3-7, *Prdx1*$^{-/-}$MEFs contained 2 to 3-fold more SA-βgal$^+$ cells compared to *Prdx1*$^{+/+}$MEFs (Figs.1B). Additionally, non-immortalized, primary MEFs lacking Prdx1 showed increased p53 expression and phosphorylation on Serine-15 after treatment with H_2O_2 for 8 h when compared to *Prdx1*$^{+/+}$MEFs (Fig. 1C). Since p38MAPKα is a major player in stress-induced senescence signaling (9, 16), we investigated if Prdx1 regulates p38MAPKα activity. We treated MEFs described above with the p38MAPKα inhibitor SB203580 and observed that the accelerated senescence in *Prdx1*$^{-/-}$MEFs is dependent on p38MAPKα activity. Shown in Figure 1D, the percent of SA-βgal$^+$ cells was significantly reduced for *Prdx1*$^{-/-}$MEFs in the presence of 6μM SB203580. *Prdx1*$^{+/+}$MEFs also demonstrated a significant decrease in SA-βgal$^+$ cells at the lower dose of 3μM SB203580. In support of this, *Prdx1*$^{-/-}$MEFs stimulated either with increasing amounts of H_2O_2 or platelet-derived growth factor (PDGF) showed higher levels of p38MAPKα phosphorylation, as well as phosphorylation of its substrate ATF-2, compared to *Prdx1*$^{+/+}$MEFs (Figs. 1E and G).

Prdx1 prevents ROS-induced senescence in breast epithelial cells

Little is known about p38MAPKα's role in senescence of breast epithelial cells. To analyze if Prdx1 regulates p38MAPKα -induced senescence in mammary epithelial cells *in vivo*, we analyzed mammary tissue from MMTV-v-H-RasV12-*Prdx1*$^{-/-}$ and MMTV-v-H-RasV12-*Prdx1*$^{+/+}$ mice (n of 7 for each genotype) for SA-βgal activity. Epithelial cells from MMTV-v-H-Ras *Prdx1*$^{-/-}$ mice consistently showed more SA-βgal positive cells compared to cells from MMTV-v-H-RasV12-*Prdx1*$^{+/+}$ mice (Fig. 2A and Table 1). Moreover, human benign (MCF-10A) and malignant (MCF-7 and MDA-MB-231) mammary epithelial cells chronically treated with H_2O_2 revealed that Prdx1 knockdown using lentiviral shPrdx1 RNA promoted H_2O_2-induced senescence, indicated by a significant increase in the number of SA-βgal$^+$-shPrdx1 cells compared to pLKO1-EV cells. In MCF-10A^{shPrdx1} cells (untreated and H_2O_2 treated) we observed a 4-5 fold increase in SA-βgal$^+$ cells compared to MCF10^{EV} cells. In MCF-7, as well as MDA-MB-231 cells, the difference was slightly smaller (1.5-2.5 fold) suggesting a higher sensitivity of untransformed cells to senescence-inducing stimuli compared to transformed cells (Figs.2B and S2A-C). This also correlated with an appearance of senescence associated cell morphology in MCF-10A^{shPrdx1} (Fig. 2SA and insets). Interestingly, treatment of MCF-7^{shPrdx1} cells with H_2O_2 resulted in a greater than 50% decrease in SA-βgal$^+$ positive cells when treated with the p38MAPKα inhibitor SB203580 compared to non-treated cells (Fig. 2C). In support of this, MCF-10A, MCF-7 as well as MDA-MB-231 cells (Fig.2B) stably expressing shPrdx1 showed significantly higher levels of H_2O_2-induced phosphorylation of p38MAPKα compared to cells expressing pLKO1-EV only (Figs. 2D-F).

Non-covalent binding of Prdx1 to MKP-1 and MKP-5 is differently modulated by H_2O_2

Prdx1 associates with PTEN, thereby protecting it from oxidation-induced inactivation and promoting its phosphatase activity (7). We therefore examined if MKP-1 and MKP-5 interact with Prdx1. We confirmed a direct binding of Prdx1 to MKP-1 and MKP-5 by coimmuneprecipitation using recombinant proteins *in vitro*. To introduce higher specificity, we included Catalase as a non-Prdx1 binding protein (Fig. 3A). A FRET-based fluorescent analysis (17) demonstrated that Prdx1's binding affinity to MKP-1 was comparable to that for PTEN (261.0 +/−21.2 nM and 247.3 +/−33.6 nM, respectively). Interestingly, Prdx1 bound to MKP-5 with an ~100-fold higher affinity (2.4 +/−0.2nM) compared to MKP-1 and PTEN (Fig. 3B). To address whether the binding was disulfide-based, we introduced tris-(2-carboxyethyl)-phosphine (TCEP) as a reducing agent to the FRET-based fluorescent analysis and found comparable K_Ds, suggesting non-covalent binding of Prdx1 with MKP-1, MKP-5 or PTEN (Table 2). To show dynamic reversibility of protein binding, we added

equal amounts of unlabeled, intact MKP-5 to MKP-5 QSY®35-labeled proteins to several points of the titration curve shown in Fig. S3A left panel ("backtitration"). This resulted in ~2x decrease of Alexa®546 quenching, indicative of a competitive binding of labeled- and unlabeled MKP-5 to the same binding site on Prdx1 (Fig. 3SA right panel). In cells, we found that under H_2O_2-induced stress, MKP-1, as PTEN(7), forms fewer complexes with Prdx1, while Prdx1:MKP-5 complexes increased Analyzing co-IPs by Western blotting in the absence of β-ME suggested that Prdx1 may bind predominantly as a dimer to MKP-1 and MKP-5 (Figs. 3C and 3D). Since Prdx1:MKP-5 complexes appeared unaffected by H_2O_2, we analyzed IPs for Prdx1-Cys52-SO3. In cells treated with H_2O_2 doses inducing Prdx1-Cys52 over-oxidation (Figs. 3C and 3D right panels), in contrast to MKP-1, Prdx1-Cys52-SO3 bound to MKP-5. To further analyze the role of Prdx1 catalytic cysteines in MKP complex formation, a Prdx1 mutant (Cys52/173Ser = Prdx1-CI) was tested by co-IP. Prdx1-CI bound to MKP-5 as Prdx1-WT did (Fig. 3F). However, although Prdx1-CI bound to MKP-1, it did not dissociate under H_2O_2 treatment in contrast to Prdx1-WT (Fig. 3J), suggesting an active role for Prdx1-Cys-52 in Prdx1:MKP-1 complex disruption.

Prdx1 protects MKP-5 from oxidation-induced oligomerization

MKP-1 and MKP-5 have been reported to undergo oxidation-induced oligomerization, reflecting MKP-1 and MKP-5 inactivity (13). Therefore, we examined if Prdx1 influences MKP-1 or MKP-5 oligomerization under H_2O_2-induced stress. 293T cells co-expressing Prdx1 with either Flag-tagged MKP-1 or MKP-5 were treated with H_2O_2 and protein lysates run under non-reducing conditions. We found that H_2O_2-induced oligomerization of MKP-1 was not prevented by exogenous Prdx1-WT (Fig. 4A), but was increased at lower H_2O_2 concentrations (25μM). This was in contrast to MKP-5, where expression of exogenous Prdx1-WT prevented H_2O_2-induced oligomerization (Fig. 4B). Interestingly, expressing Prdx1-CI increased H_2O_2-induced oligomerization of MKP-5 but not of MKP-1 (Figs. 4C and 4D). Analysis of p38MAPKα phosphorylation revealed that exogenous Prdx1-WT supported MKP-5 mediated p38MAPKα dephosphorylation, particularly at higher H_2O_2 concentrations (100 and 250μM) in contrast to Prdx1-CI (Figs. 4F, 4H and 4J). This was in contrast to MKP-1, where co-expression with exogenous Prdx1-WT slightly increased p38MAPKα phosphorylation, while Prdx1-CI decreased it (Figs. 4E, 4G and 4I).

In the presence of H_2O_2 Prdx1 decreases MKP-1, but protects and enhances MKP-5 catalytic activity

To confirm that Prdx1 inhibits MKP-1 catalytic activity under H_2O_2-induced stress, but promotes MKP-5 catalytic activity, we measured recombinant MKP-1 and MKP-5-mediated hydrolysis of 6,8-difluoro-4-methylumbelliferyl phosphate (DiFMUP) (18) in the presence and absence of Prdx1 and H_2O_2. A substrate concentration of 160 μM DiFMUP was determined optimal.. As shown in Fig. 5A, MKP-1 maintains its activity towards DiFMUP better over time compared to MKP-5. Interestingly, recombinant MKP-1 was inactivated by 50 or 150 μM of H_2O_2 only when Prdx1 was present, but not in its absence (Fig. 5B). In contrast, the H_2O_2-induced decrease of MKP-5 activity was improved significantly in the presence of Prdx1 (Fig. 5C). Using a random effects model comparing the effect of Prdx1 on MKP-1 activity, the six tests of differences in treatment effects (Prdx1) over time were all statistically significant at the $\alpha = 0.05$ level (Figs. 5B and C).

Prdx1 prevents ROS-induced senescence in MCF-7 cells through MKP-5 activity

Flag-MKP-1 WT or CI (catalytically inactive mutant) and Flag-MKP-5 WT or CI mutants were expressed in MCF-7 cells and analyzed for SA-βgal activity after H_2O_2 treatment; these are subsequently referred to as MKP-1 or MKP-5-cells. Shown in Fig. 6A, after H_2O_2-treatment, MKP-5-^{WT}-cells had an 80% decrease in SA-βgal activity compared to EV-cells or MKP-5^{CI}-cells. Interestingly, expression of both MKP-1^{WT} and MKP-1^{CI} decreased

senescence by 50% compared to EV-cells. No quantitative difference of SA-βgal$^+$ was found between MKP-1^{WT} and MKP-1^{CI} cells. As expected, in untreated cells, expression of MKP-5^{CI} and MKP-1^{CI} increased p38MAPKα TGY-phosphorylation, whereas expression of MKP-1^{WT} and MKP-5^{WT} decreased it. Additionally, , expression of MKP-5^{WT} decreased p38MAPKα phosphorylation in H_2O_2-treated cells, where MKP-1^{WT} did not. . Interestingly, expression of MKP-5^{WT}, and to a lesser extent MKP-5^{CI},revealed a slower migrating band identified as p38MAPKδ (Fig. 6B). Surprisingly, expression of MKP-1^{WT} or MKP-5^{WT} had very little effect on decreasing phosphorylation of JNK proteins, although expression of MKP-1^{CI} increased JNK phosphorylation independent of H_2O_2 treatment.To analyze delayed JNK activation, we examined MCF-7 clones two days after H_2O_2 treatment. We found that MKP-1^{WT} suppressed JNK activity and PARP cleavage (data not shown). Lastly, we investigated if the senescence observed in Fig. 6A results in tumor suppression in a soft agar assay. As shown in Fig. 6C, expression of MKP-5^{CI} decreased colony formation of MCF-7^{EV} cells by 50%. Surprisingly, expressing MKP-1^{WT} showed a comparable decrease, while MKP-1^{CI} and MKP-5^{WT} expression resulted in slightly increased colony formation compared to MCF-7^{EV} cells.

Discussion

While it is widely accepted that oxidation-induced posttranslational protein modifications contribute to cell signaling, more studies are needed to fully understand how protein oxidation orchestrates signaling events. As mentioned, we have shown that Prdx1 protects the redox-sensitive PTEN from oxidation-induced inactivation (7). In the past, senescence has mainly been viewed as a tumor suppressive mechanism and more recently its therapeutic implications are investigated. Given that ROS induce senescence, and loss of Prdx1 promotes a p38MAPKα-dependent senescent phenotype, we sought to determine whether Prdx1 regulates senescence signaling specifically through the redox-sensitive p38MAPKα phosphatases, MKP-1 and MKP-5.

A role for Prdx1 in senescence

Loss of Prdx1 accelerated the processes of senescence in MEFs (Figs. 1A and B). This was not surprising given that a similar phenotype has been described for Prdx2 (19), which shares high homology with Prdx1. Thus, Prdx1 loss amplified H_2O_2-induced p53 Ser19 phosphorylation (Fig. 1C), known to accompany persistent DNA-damage (20). The latter can be found in *Prdx1*$^{-/-}$MEFs (14) and is believed to trigger the senescence-associated secretory phenotype (SASP) (21). Our data suggest that Prdx1 suppresses p38MAPKα activation in the process of spontaneous immortalization, since SB203580, an ATP competitor for the p38MAPKα/β ATP docking site and known inhibitor of ROS and oncogene-induced senescence (9, 22-24), could inhibit the processes of senescence in *Prdx1*$^{-/-}$MEFs (Fig.1D). Moreover, PDGF treatment augmented p38MAPKα activity in *Prdx1*$^{-/-}$ MEFs, supporting the notion that growth factor signaling stimulates H_2O_2 production via NADPH oxidases (1), which have recently been implicated to mediate oncogenic-induced senescence (25, 26).

Prdx1 as a sensor for p38MAPK signaling

Our novel findings suggest Prdx1 acts as an inhibitor of p38MAPKα-mediated senescence, since its loss promoted H_2O_2- induced senescence in various cell types *in vivo* and *in vitro* in a p38MAPKα–dependent manner (Fig. 2C). Interestingly, the largest increase in SA-βgal$^+$ cells due to the loss of Prdx1 was seen in the benign MCF-10A cells (Fig. 2B). This indicated to us a) that Prdx1's regulatory role in senescence may be more prominent in non-transformed and b) that cancer cells may not respond to p38MAPKα signaling the way benign cells do. An uncoupling of p38MAPKα apoptotic signaling under conditions of high

cellular ROS was recently suggested. P38MAPKα was found to mediate ROS-dependent pro-apoptotic/anti-oncogenic effects mostly in cells with high p38MAPKα activity and low ROS levels, and not in cancer cells with less p38MAPKα activation, but higher ROS levels (27). Considering that cancer cells contain higher levels of ROS compared to normal cells, p38MAPKα signaling may differ in benign compared to malignant cells. Our data suggest that such specific ROS-dependent regulation of cell signaling exists since we describe that the over-oxidation of Prdx1's peroxidatic Cys52 to sulfonic acid differentially modulated MKP-1 and MKP-5.. Such a hypothesis excludes the possibility that Prdx1's direct binding to MKP-1 or MKP-5 (Fig. 3A) is disulfide-based, involving Cys52. Our data support this given the observation that addition of a reducing agent (TCEP) in the FRET-based fluorescent analysis resulted in comparable K_Ds: for MKP-5 and for MKP-1 (Fig. 3SA and Table 2). Moreover, although Prdx1 bound to MKP-5 with a higher binding affinity than MKP-1 (Fig. 3A), adding equal amounts of unlabeled intact MKP-5 to MKP-5 QSY®35-labeled proteins showed dynamic reversibility of protein binding (Fig. 3SB). The idea that cysteine oxidation regulates signal transduction is not new (28), however, additional specific examples are needed. We demonstrate that under increasing doses of H_2O_2, Prdx1:MKP-1 complexes dramatically decreased and did not contain any detectable over-oxidized Prdx1 (Fig. 3C), whereas MKP-5 increasingly associated with overoxidized Prdx1 (Fig. 3D). Moreover, in contrast to Prdx1-WT, Prdx1-CI binding to MKP-1 was unaffected by H_2O_2 (Fig. 3E) whereas MKP-5 binding to Prdx1-CI was comparable to Prdx1-WT (Fig. 3F). Although these findings suggest that the process of Cys52 over-oxidation may actively contribute to the dissociation of Prdx1 from MKP-1, other active cysteines of Prdx1, including Cys83, may prevent dissociation of Prdx1 from MKP-1. Further studies are needed to address this question.

MKP-1 and MKP-5 expression is induced by various ROS-inducing stimuli (29-32) (33, 34), and both are inactivated by ROS due to oxidation of their catalytic cysteines, coinciding with formation of oligomeric structures (13, 29, 35, 36). Prdx1 preferentially prevented MKP-5 oxidation-induced oligomerization under conditions where Prdx1:MKP-5 complexes were formed. Moreover, protection of MKP-5 by Prdx1 translated into enhanced phosphatase activity, even under high concentrations of H_2O_2 (100 and 250μM), as p38MAPKα-phosphorylation was decreased in the presence of exogenous Prdx1 (Fig. 4F). Interestingly, Prdx1-CI, although bound to MKP-5 under H_2O_2-induced stress, had little influence on preventing MKP-5 oligomerization (Fig. 4D) or reversing p38MAPKα dephosphorylation (Fig. 4F). In fact, Prdx1-CI compromised MKP-5 activity towards p38MAPKα, which was especially pronounced in samples treated with higher H_2O_2 amounts (Figure 4F, 4H and 4J). Considering our binding data, this suggests that over-oxidation of Prdx1-Cys52 preserves MKP-5 activity towards p38MAPKα and prevents its oxidation-induced oligomerization. In contrast to MKP-5, higher concentrations of H_2O_2 (100 to 250μM) decreased Prdx1:MKP-1 complex formation(Fig. 3C), leaving Prdx1 unable to protect MKP-1 from oxidation-induced oligomerization, thereby blunting MKP-1 activity towards p38MAPKα. Actually, under conditions of lower H_2O_2 concentrations (25-100μM), we found that Prdx1 WT increased MKP-1 oligomerization, whereas Prdx1-CI, which still binds to MKP-1 under H_2O_2-induced stress, appeared to protect MKP-1 from oligomer formation (Fig. 4C). Interestingly, this translated into less dephosphorylation of p38MAPKα when MKP-1 was co-expressed with Prdx1 WT compared to co-expression with Prdx1-CI (Figs. 4E,G and I). Supporting this, MKP-1 phosphatase activity towards DiFMUP was decreased only in the presence of Prdx1 after H_2O_2 treatment (Fig. 5B), although several studies have described that MKP-1 is readily over-oxidized and inactivated by ROS (29, 37). This suggests that a) under non-H_2O_2-conditions Prdx1 promotes MKP-1 activity, whereas under H_2O_2-induced stress Prdx1 inactivates MKP-1, and b) it is unlikely that Prdx1 competes with p38MAPKα for MKP-1 binding (38-40). Little is known about how MKP-5 reacts to oxidative stress. Our data suggest that recombinant MKP-5 phosphatase activity is

decreased by H_2O_2 in a dose-dependent manner, and the presence of Prdx1 protected and even slightly enhanced MKP-5 activity.

Taken together, we describe that over-oxidation of Prdx1's peroxidatic cysteine adjusts MKP-1 and MKP-5 activity in an H_2O_2-dependent manner, thereby regulating p38MAPKα activity. Given the diversity of p38MAPKα signaling, such regulation may be meaningful for redox-stress signaling. In this context, our data may support recent findings published by the Veal lab, where in an elegant study the over-oxidation of yeast Prdx Tpx1 was found critical for thioredoxin-mediated repair of oxidized proteins. In essence, this study proposed that in an environment of elevated oxidative stress, where Prdx Tpx1 is found over-oxidized and therefore “non-reducible” by thioredoxin, cell survival is promoted through protein repair by the available thioredoxin (41). Given our data, we suspect that MKP-5 is perhaps a thioredoxin substrate. This needs to be examined in the future.

A specific role for Prdx1 as a promoter of MKP-5 activity in p38MAPK signaling in breast cancer senescence

To date, no role for MKP-1 or MKP-5 in breast cancer or senescence hast been established. MKP-5 has been implicated in prostate cancer, as a Vitamin-D-inducible gene, which indirectly inhibits secretion of pro-carcinogenic inflammatory factors including IL-6, a key player in SASP (42), through blocking p38MAPKα signaling (43). Our data support this, since MKP-5^{WT} was a potent inhibitor of H_2O_2-induced senescence in MCF-7 cells, where MKP-5^{CI} was not (Fig. 6A). MCF-7 cells expressing MKP-1^{WT} or MKP-1^{CI} showed equal suppression of senescence, but no differences in the amount of p38MAPKα phosphorylation, suggesting that Prdx1 regulates MKP-1 activity towards p38MAPKα (Fig. 6B). Whether MKP-1-CI can bind to p38MAPKα needs to be determined. Recent work demonstrated that MKP-1 overexpression in MCF-7 cells prevents H_2O_2-induced cell death. Since MCF-7 cells express endogenous Prdx1, this difference is perhaps due to the high dose of H_2O_2 (300 μM) given, where Prdx1 is most likely over-oxidized and less available to bind to MKP-1, thereby freeing MKP-1 to dephosphorylate p38 and JNK (44).

MKP-1 and MKP-5 specificity is towards p38MAPKα/β, and not p38MAPKδ/γ (45). Interestingly, treating MCF-7 cells with 25 μM H_2O_2 revealed a slower migrating band only in cells expressing MKP-5^{WT} and to a lesser extent MKP-5^{CI} (Fig. 6B). This band was detected with anti- p38MAPKδ , not anti-p38MAPKα antibody, , suggesting a novel role for p38MAPKδ in senescence. This idea fits, given that p38MAPKδ activity seemingly promotes oncogenesis (46), and MCF-7-MKP-5^{WT} formed ~2.5 fold more colonies in soft agar compared MCF-7-MKP-5^{CI} cells (Fig. 6C). Therefore, perhaps suppression of p38MAPKα represses senescence and promotes oncogenesis by p38MAPKδ activation. Expression of MKP-1^{WT} also led to a reduction in colony numbers, compared to MCF-7-MKP-1^{CI} cells. This may be because JNK is essential for MCF-7 proliferation, since knockdown of JNK in MCF-7 cells inhibited MCF-7 proliferation (47); overexpression of MKP-1, often referred to as the “JNK phosphatase” (48), may have a similar effect.

In summary, our data suggest that under normal ROS homeostasis, Prdx1 promotes MKP-1 and MKP-5 activity (Fig. 7). Under increasing ROS levels, Prdx1 becomes over-oxidized on its peroxidatic cysteine Cys52, Prdx1-Cys52-SO3 forms less Prdx1/MKP-1 complexes leading to MKP-1 inactivation and p38MAPKα activation. Conversely,Prdx1-Cys52-SO3 binds to MKP-5 and preserves MKP-5 activity, ensuring p38MAPKα inhibition. We speculate that activation of MKP-5 insensitive p38MAPK isoforms or JNK signaling may become activated and induce cancer-associated senescence. Clearly, further studies are needed to address this. Collectively, our findings provide compelling novel evidence that the peroxidatic cysteine Cys52 of Prdx1 serves as a sensor in ROS-signaling, expanding the function of Prdx1 beyond its peroxidase activity.

Material and Methods

Reagents and Cell Culture

All chemicals, including 5-Bromo-4-chloro-3-indolyl β- D-galactopyranoside, Flag-agarose conjugated beads, and recombinant Prdx1 protein were purchased from Sigma Aldrich unless otherwise noted. Antibodies against pan p38, p-p38 (Thr180/Tyr182), p-ATF2 (Thr69/71), MKP-5, HA-tag, and Flag-tag were purchased from Cell Signaling. Actin was purchased from Chemicon, antibodies recognizing Prdx1 and Prdx1-SO_3 were purchased through Abcam, and MKP-1 from Santa Cruz. Recombinant MKP-1 and MKP-5 proteins were purchased from Enzo Life Sciences. Materials for cell culture medium including DMEM, FBS, Glutamax, NEAA, sodium pyruvate, Pen/Strep, insulin, DMEM without Phenol Red, PBS, and PDGF were purchased from Invitrogen. MEFs were generated from $Prdx1^{+/-}$ mice as described (7), MCF-10A, MDA-MB-231, and MCF-7 cells were maintained as described (49, 50).

Constructs

Expression vectors used for 293T/17 (ATCC) transfections included: Flag- p38MAPKα in pcDNA3.1, HA-Prdx1 (WT and mutant) in PCGN, Flag-MKP1/5 in pQCXIP (WT and mutant), and Myc-WT-MKP-5 in pSRα expression vector. The MKP-5 mutant was constructed by PCR-based mutagenesis (Stratagene). Flag-MKP-1/5 (both WT and mutants) were cloned into AgeI/BamHI of pQCXIP, and used for both 293T experiments, as well as making retrovirus for infection of MCF-7 cells. The expression plasmid pLKO.1 was used for shPrdx1.

MEF Oxidative Stress Experiments

$Prdx1^{-/-}$ and $Prdx1^{+/+}$MEFs were serum-starved in 0.25% FBS for 48 h before treatment. Cells were either treated with PDGF in phenol-free DMEM supplemented with 0.1% BSA or with increasing doses (25-200 μM) of H_2O_2 in serum-free DMEM for 10 min. Cell lysate was processed as previously described (7).

Co-Immunoprecipitation Studies

293T/17 (ATCC) cells were transfected with various constructs as described (7). For coimmunoprecipitation 750-1000 μg of protein was subjected to immunoprecipitation using Anti-FLAG M2 affinity gel. Affinity matrix was harvested by centrifugation at 3000xg for 2 min and washed three times. The resin was re-suspended in reducing SDS-PAGE loading buffer, boiled 10 min, and analyzed by SDS-PAGE/ Western Blotting.

Prdx1:MKP Pulldown

MKP-1/5 recombinant proteins were incubated with equimolar concentrations (100 nM) of Prdx1 overnight at 4°C in buffer containing 20 mM Hepes (pH 8.0), 150 mM NaCl, 2 mM $MgCl_2$, 1 mM DTT, 50 μM PMSF, 5 mM benzamidine hydrochloride, 3 μM aprotinin and 1% Triton X-100. Recombinant proteins were added to 50μl of Prdx1 conjugated Protein G agarose matrix, and allowed to incubate at 4°C for 1 hr. The resin was then harvested and washed as above. Proteins were eluted with reducing SDS loading buffer, boiled for 10 min, and analyzed by SDS-PAGE/Western Blotting.

Fluorescent Kd Analysis

Prdx1 protein was incubated with succinimidylester of Alexa Fluor® 546 carboxylic acid (Invitrogen) and purified MKP proteins were incubated with succinimidylester of QSY® 35 acetic acid (Invitrogen, both at 5x excess to protein) at RT overnight under constant agitation to label primary amines according to manufacturer recommendations. The reaction

mixtures were processed using BioSpin 6 (BioRad) size-exclusion spin column to remove unreacted dyes and exchange reaction buffers to PBS (pH=7.4). The resultant labeled protein concentration was analyzed with standard Bradford assay (BioRad). The analysis is based on quenching of Alexa 546 fluorescence by QSY 35 (the distance of 50% quenching is ~25 Å), and was performed as previously described (17). The Kd is a concentration of 50% Alexa 546 emission decrease.

Recombinant MKP-1 and MKP-5 Phosphatase Assay

Recombinant MKP-1 and MKP-5 phosphatase activity was analyzed in the presence and absence of Prdx1 under increasing H_2O_2 stress using the EnzChek® Phosphatase Assay Kit from Molecular Probes. Various concentrations (80μM – 320 μM) of the substrate 6,8-difluoro-4-methylumbelliferyl (DiFMUP) were used to asses the activity of MKP-1 and MKP-5 (30pmols each in 200μl reaction buffer) over 2 h, before deciding on 160μM DiFMUP for all experiments. Using a 1:1 molar ratio of MKP:Prdx1, proteins were pipetted into a black, clear-bottom 96-well plate (Costar) following addition of H_2O_2, and hydrolysis of DiFMUP was measured at ~360/460 nm using a fluorescence plate reader.

H_2O_2 - Induced Stress and Senescence in MCF-10A, MCF-7, and MDA-MB-231 Cells

For detection of p38MAPKα phosphorylation, cells were plated at 8.0 x 10^4 overnight. The following day, media was removed and replaced with serum-free DMEM for 2 hrs before cells were treated with H_2O_2 and lysed with 150 μl of lysis buffer (7). Cell lysate was prepared and 80 μg was analyzed on 10% SDS gels. For H_2O_2-induced senescence, cells were plated in 6-well plates overnight, and treated with H_2O_2 for 4 days. Following treatment, cells were passaged into fresh medium for 24 h and sub-cultured at low confluency for 10 days. Cells were stained as described (51), and postitive cells were counted by light microscopy.

SA-βgal-staining of MMTV-H-Ras mammary glands

Mammary glands were immediately sliced into small pieces (0.5 cm × 0.5 cm) and snap frozen in liquid N2 after collection. Tissue pieces were fixed in glutaraldehyde o/n before incubation in β-gal solution o/n, embedded in paraffin, and processed for histological analysis.

Virus Production

Phoenix cells were plated at 0.4 × 10^6 in 6cm dishes in DMEM overnight for retrovirus production of Flag-MKP1/5 in pQCXIP (WT and mutant). Cells were transfected with MKP constructs, VSV-G, and gagPol expressing plasmids using FuGENE 6 (as stated above). MCF-7 cells were infected with filtered retroviral supernatant with addition of 8μg/ml polybrene for 4-6 h before selection in puromycin. To make shPrdx1 lentivirus, 293T/17 (ATCC) cells were plated as above. The following day, cells were transfected with 1μg of either shPrdx1 or empty vector (EV) pLKO.1 with pDM2.G and psPAX2 expressing plasmids. Twenty-four h virus was harvested and filtered, and cells were infected overnight. The following day, virus was removed and replaced with appropriate medium. Cells were selected with puromycin and checked for knockdown by SDS-PAGE/Western Blotting.

Supplementary Material

Refer to Web version on PubMed Central for supplementary material.

Acknowledgments

We would like to thank Dr. Eisuke Nishida for providing the MKP-5 cDNA, Yusen Liu for providing MKP-1 WT and MKP-1 C258S cDNA, and Steve Rosenzweig and Scott Eblen for fruitful discussions. This work has been funded by K22 ES012985-01 (C.A.N), W81XWH-07-1-0691 (C.A.N.), R01 CA131350 (C.A.N) and 5T32CA119945-05 (B.T.).

References

1. Rhee SG. Cell signaling. H2O2, a necessary evil for cell signaling. science. Jun 30; 2006 312(5782): 1882–3. [PubMed: 16809515]
2. Claiborne A, Yeh JI, Mallett TC, Luba J, Crane EJ 3rd, Charrier V, et al. Protein-sulfenic acids: diverse roles for an unlikely player in enzyme catalysis and redox regulation. Biochemistry. Nov 23; 1999 38(47):15407–16. [PubMed: 10569923]
3. Neumann CA, Fang Q. Are peroxiredoxins tumor suppressors? Curr Opin Pharmacol. Aug; 2007 7(4):375–80. [PubMed: 17616437]
4. Neumann CA, Cao J, Manevich Y. Peroxiredoxin 1 and its role in cell signaling. Cell Cycle. Dec 15; 2009 8(24):4072–8. [PubMed: 19923889]
5. Kim YJ, Lee WS, Ip C, Chae HZ, Park EM, Park YM. Prx1 suppresses radiation-induced c-Jun NH2-terminal kinase signaling in lung cancer cells through interaction with the glutathione S-transferase Pi/c-Jun NH2-terminal kinase complex. Cancer Res. Jul 15; 2006 66(14):7136–42. [PubMed: 16849559]
6. Neumann CA, Wen ST, Van Etten RA. Role of the c-Abl tyrosine kinase in the cellular response to oxidative stress. Blood. 1998; 92(10)
7. Cao J, Schulte J, Knight A, Leslie NR, Zagozdzon A, Bronson R, et al. Prdx1 inhibits tumorigenesis via regulating PTEN/AKT activity. EMBO J. Apr 16.2009
8. Han J, Sun P. The pathways to tumor suppression via route p38. Trends Biochem Sci. Aug; 2007 32(8):364–71. [PubMed: 17624785]
9. Wang W, Chen JX, Liao R, Deng Q, Zhou JJ, Huang S, et al. Sequential activation of the MEK-extracellular signal-regulated kinase and MKK3/6-p38 mitogen-activated protein kinase pathways mediates oncogenic ras-induced premature senescence. Mol Cell Biol. May; 2002 22(10):3389–403. [PubMed: 11971971]
10. Tonks NK. Protein tyrosine phosphatases: from genes, to function, to disease. Nat Rev Mol Cell Biol. Nov; 2006 7(11):833–46. [PubMed: 17057753]
11. Peters GH, Frimurer TM, Olsen OH. Electrostatic evaluation of the signature motif (H/V)CX5R(S/T) in protein-tyrosine phosphatases. Biochemistry. Apr 21; 1998 37(16):5383–93. [PubMed: 9548920]
12. Tonks NK. Redox redux: revisiting PTPs and the control of cell signaling. Cell. Jun 3; 2005 121(5):667–70. [PubMed: 15935753]
13. Kamata H, Honda S, Maeda S, Chang L, Hirata H, Karin M. Reactive oxygen species promote TNFalpha-induced death and sustained JNK activation by inhibiting MAP kinase phosphatases. Cell. Mar 11; 2005 120(5):649–61. [PubMed: 15766528]
14. Neumann CA, Krause DS, Carman CV, Das S, Devendra D, Abraham JL, et al. Essential role for the peroxiredoxin Prdx1 in erythrocyte antioxidant defense and tumor suppression. Nature. 2003; 424:561–5. [PubMed: 12891360]
15. Todaro GJ, Green H. Quantitative studies of the growth of mouse embryo cells in culture and their development into established lines. Journal of Cell Biology. 1963; 17:299–313. [PubMed: 13985244]
16. Iwasa H, Han J, Ishikawa F. Mitogen-activated protein kinase p38 defines the common senescence-signalling pathway. Genes Cells. Feb; 2003 8(2):131–44. [PubMed: 12581156]
17. Bowers RR, Manevich Y, Townsend DM, Tew KD. Sulfiredoxin Redox-Sensitive Interaction with S100A4 and Non-Muscle Myosin IIA Regulates Cancer Cell Motility. Biochemistry. Oct 2; 2012 51(39):7740–54. [PubMed: 22934964]
18. Jeong DG, Yoon TS, Kim JH, Shim MY, Jung SK, Son JH, et al. Crystal structure of the catalytic domain of human MAP kinase phosphatase 5: structural insight into constitutively active

phosphatase. J Mol Biol. Jul 28; 2006 360(5):946–55. [PubMed: 16806267] [Research Support, Non-U.S. Gov't].

19. Han YH, Kim H, Kim J, Kim S, Yu D, Moon EY. Inhibitory role of peroxiredoxin II (PrxII) on cellular senescence. FEBS. 2005; 579:4897–902.
20. Kuilman T, Michaloglou C, Mooi WJ, Peeper DS. The essence of senescence. Genes Dev. Nov 15; 2010 24(22):2463–79. [PubMed: 21078816]
21. Rodier F, Coppe JP, Patil CK, Hoeijmakers WA, Munoz DP, Raza SR, et al. Persistent DNA damage signalling triggers senescence-associated inflammatory cytokine secretion. Nat Cell Biol. Aug; 2009 11(8):973–9. [PubMed: 19597488]
22. Coulthard LR, White DE, Jones DL, McDermott MF, Burchill SA. p38(MAPK): stress responses from molecular mechanisms to therapeutics. Trends Mol Med. Aug; 2009 15(8):369–79. [PubMed: 19665431]
23. Trost TM, Lausch EU, Fees SA, Schmitt S, Enklaar T, Reutzel D, et al. Premature senescence is a primary fail-safe mechanism of ERBB2-driven tumorigenesis in breast carcinoma cells. Cancer Res. Feb 1; 2005 65(3):840–9. [PubMed: 15705882]
24. Lee JJ, Lee JH, Ko YG, Hong SI, Lee JS. Prevention of premature senescence requires JNK regulation of Bcl-2 and reactive oxygen species. Oncogene. Jan 28; 2009 29(4):561–75. [PubMed: 19855432]
25. Schilder YD, Heiss EH, Schachner D, Ziegler J, Reznicek G, Sorescu D, et al. NADPH oxidases 1 and 4 mediate cellular senescence induced by resveratrol in human endothelial cells. Free radical biology & medicine. Jun 15; 2009 46(12):1598–606. [PubMed: 19328228] [Research Support, N.I.H., Extramural Research Support, Non-U.S. Gov't].
26. Weyemi U, Lagente-Chevallier O, Boufraqech M, Prenois F, Courtin F, Caillou B, et al. ROS-generating NADPH oxidase NOX4 is a critical mediator in oncogenic H-Ras-induced DNA damage and subsequent senescence. Oncogene. Aug 15.2011
27. Dolado I, Swat A, Ajenjo N, De Vita G, Cuadrado A, Nebreda AR. p38alpha MAP kinase as a sensor of reactive oxygen species in tumorigenesis. Cancer Cell. Feb; 2007 11(2):191–205. [PubMed: 17292829]
28. Cross JV, Templeton DJ. Regulation of signal transduction through protein cysteine oxidation. Antioxid Redox Signal. Sep-Oct;2006 8(9-10):1819–27. [Review]. [PubMed: 16987034]
29. Hou N, Torii S, Saito N, Hosaka M, Takeuchi T. Reactive oxygen species-mediated pancreatic beta-cell death is regulated by interactions between stress-activated protein kinases, p38 and c-Jun N-terminal kinase, and mitogen-activated protein kinase phosphatases. Endocrinology. Apr; 2008 149(4):1654–65. [PubMed: 18187551]
30. Nonn L, Duong D, Peehl DM. Chemopreventive anti-inflammatory activities of curcumin and other phytochemicals mediated by MAP kinase phosphatase-5 in prostate cells. Carcinogenesis. Jun; 2007 28(6):1188–96. [PubMed: 17151092] [Research Support, U.S. Gov't, Non-P.H.S.].
31. Tephly LA, Carter AB. Differential expression and oxidation of MKP-1 modulates TNF-alpha gene expression. American journal of respiratory cell and molecular biology. Sep; 2007 37(3): 366–74. [PubMed: 17507666] [In Vitro Research Support, Non-U.S. Gov't Research Support, U.S. Gov't, Non-P.H.S.].
32. Dasgupta J, Kar S, Liu R, Joseph J, Kalyanaraman B, Remington SJ, et al. Reactive oxygen species control senescence-associated matrix metalloproteinase-1 through c-Jun-N-terminal kinase. Journal of cellular physiology. Oct; 2010 225(1):52–62. [PubMed: 20648623] [Research Support, N.I.H., Extramural Research Support, Non-U.S. Gov't].
33. Bar-Shira A, Rashi-Elkeles S, Zlochover L, Moyal L, Smorodinsky NI, Seger R, et al. ATM-dependent activation of the gene encoding MAP kinase phosphatase 5 by radiomimetic DNA damage. Oncogene. Jan 24; 2002 21(5):849–55. [PubMed: 11850813] [Research Support, Non-U.S. Gov't Research Support, U.S. Gov't, P.H.S.].
34. Wang Z, Cao N, Nantajit D, Fan M, Liu Y, Li JJ. Mitogen-activated protein kinase phosphatase- 1 represses c-Jun NH2-terminal kinase-mediated apoptosis via NF-kappaB regulation. The Journal of biological chemistry. Jul 25; 2008 283(30):21011–23. [PubMed: 18508759] [Research Support, N.I.H., Extramural].

35. Staples CJ, Owens DM, Maier JV, Cato AC, Keyse SM. Cross-talk between the p38alpha and JNK MAPK pathways mediated by MAP kinase phosphatase-1 determines cellular sensitivity to UV radiation. J Biol Chem. Aug 20; 2010 285(34):25928–40. [PubMed: 20547488]
36. Tephly LA, Carter AB. Differential expression and oxidation of MKP-1 modulates TNF-alpha gene expression. Am J Respir Cell Mol Biol. Sep; 2007 37(3):366–74. [PubMed: 17507666]
37. Dasgupta J, Kar S, Liu R, Joseph J, Kalyanaraman B, Remington SJ, et al. Reactive oxygen species control senescence-associated matrix metalloproteinase-1 through c-Jun-N-terminal kinase. J Cell Physiol. Oct; 2010 225(1):52–62. [PubMed: 20648623]
38. Hutter D, Chen P, Barnes J, Liu Y. Catalytic activation of mitogen-activated protein (MAP) kinase phosphatase-1 by binding to p38 MAP kinase: critical role of the p38 C-terminal domain in its negative regulation. Biochem J. Nov 15; 2000 352(Pt 1):155–63. [PubMed: 11062068]
39. Slack DN, Seternes OM, Gabrielsen M, Keyse SM. Distinct binding determinants for ERK2/p38alpha and JNK map kinases mediate catalytic activation and substrate selectivity of map kinase phosphatase-1. J Biol Chem. May 11; 2001 276(19):16491–500. [PubMed: 11278799]
40. Tanoue T, Maeda R, Adachi M, Nishida E. Identification of a docking groove on ERK and p38 MAP kinases that regulates the specificity of docking interactions. EMBO J. Feb 1; 2001 20(3):466–79. [PubMed: 11157753]
41. Day AM, Brown JD, Taylor SR, Rand JD, Morgan BA, Veal EA. Inactivation of a peroxiredoxin by hydrogen peroxide is critical for thioredoxin-mediated repair of oxidized proteins and cell survival. Molecular cell. Feb 10; 2012 45(3):398–408. [PubMed: 22245228] [Research Support, Non-U.S. Gov't].
42. Coppe JP, Patil CK, Rodier F, Krtolica A, Beausejour CM, Parrinello S, et al. A human-like senescence-associated secretory phenotype is conserved in mouse cells dependent on physiological oxygen. PLoS One. 2010; 5(2):e9188. [PubMed: 20169192]
43. Nonn L, Peng L, Feldman D, Peehl DM. Inhibition of p38 by vitamin D reduces interleukin-6 production in normal prostate cells via mitogen-activated protein kinase phosphatase 5: implications for prostate cancer prevention by vitamin D. Cancer Res. Apr 15; 2006 66(8):4516–24. [PubMed: 16618780]
44. Zhou JY, Liu Y, Wu GS. The role of mitogen-activated protein kinase phosphatase-1 in oxidative damage-induced cell death. Cancer research. May 1; 2006 66(9):4888–94. [PubMed: 16651445] [Research Support, N.I.H., Extramural Research Support, Non-U.S. Gov't].
45. Tanoue T, Yamamoto T, Maeda R, Nishida E. A Novel MAPK phosphatase MKP-7 acts preferentially on JNK/SAPK and p38 alpha and beta MAPKs. J Biol Chem. Jul 13; 2001 276(28):26629–39. [PubMed: 11359773]
46. Schindler EM, Hindes A, Gribben EL, Burns CJ, Yin Y, Lin MH, et al. p38delta Mitogen-activated protein kinase is essential for skin tumor development in mice. Cancer research. Jun 1; 2009 69(11):4648–55. [PubMed: 19458068] [Research Support, Non-U.S. Gov't].
47. Parra E, Ferreira J. Knockdown of the c-Jun-N-terminal kinase expression by siRNA inhibits MCF-7 breast carcinoma cell line growth. Oncol Rep. Nov; 2010 24(5):1339–45. [PubMed: 20878129] [Research Support, Non-U.S. Gov't].
48. Liu Y, Gorospe M, Yang C, Holbrook NJ. Role of mitogen-activated protein kinase phosphatase during the cellular response to genotoxic stress. Inhibition of c-Jun N-terminal kinase activity and AP-1- dependent gene activation. The Journal of biological chemistry. Apr 14; 1995 270(15):8377–80. [PubMed: 7721728]
49. Debnath J, Muthuswamy SK, Brugge JS. Morphogenesis and oncogenesis of MCF-10A mammary epithelial acini grown in three-dimensional basement membrane cultures. Methods. Jul; 2003 30(3):256–68. [PubMed: 12798140]
50. Dasari A, Bartholomew JN, Volonte D, Galbiati F. Oxidative stress induces premature senescence by stimulating caveolin-1 gene transcription through p38 mitogen-activated protein kinase/Sp1-mediated activation of two GC-rich promoter elements. Cancer Res. Nov 15; 2006 66(22):10805–14. [PubMed: 17108117]
51. Dimri GP, Lee X, Basile G, Acosta M, Scott G, Roskelley C, et al. A biomarker that identifies senescent human cells in culture and aging skin in vivo. PNAS. 1995; 92:9363–7. [PubMed: 7568133]

52. Wang Z, Cao N, Nantajit D, Fan M, Liu Y, Li JJ. Mitogen-activated protein kinase phosphatase-1 represses c-Jun NH2-terminal kinase-mediated apoptosis via NF-kappaB regulation. J Biol Chem. Jul 25; 2008 283(30):21011–23. [PubMed: 18508759]

53. Theodosiou A, Smith A, Gillieron C, Arkinstall S, Ashworth A. MKP5, a new member of the MAP kinase phosphatase family, which selectively dephosphorylates stress-activated kinases. Oncogene. Nov 25; 1999 18(50):6981–8. [PubMed: 10597297] [Research Support, Non-U.S. Gov't].

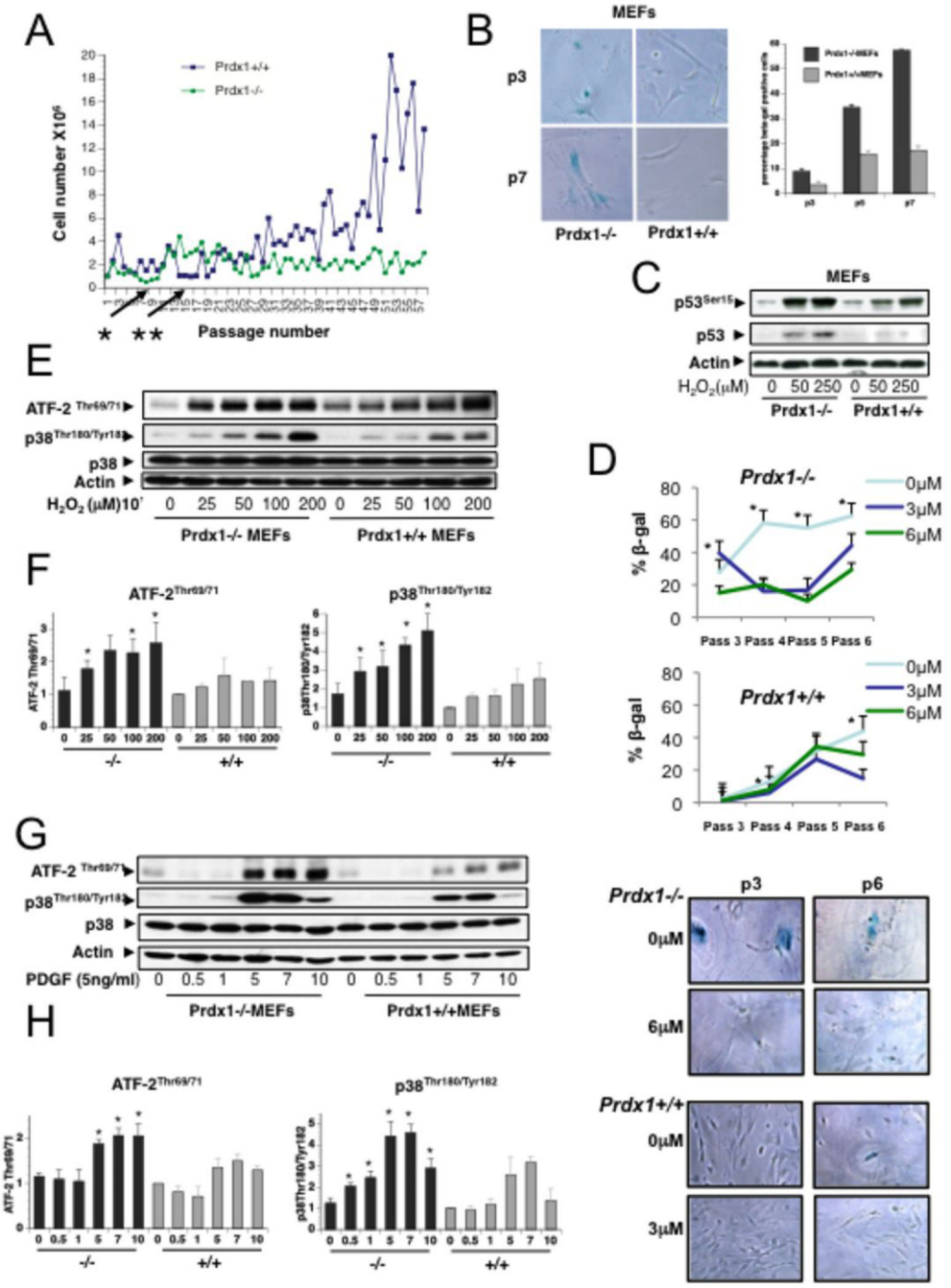

Figure 1. Lack of Prdx1 promotes senescence in murine fibroblasts and mammary epithelial cells

A. Primary Prdx1$^{-/-}$ and $^{+/+}$MEFs were immortalized following the 3T3 protocol. Cells were counted every three days and cell numbers were plotted on the y-Axis; passages were plotted on the x-axis. Arrows indicate senescence: cell numbers did not exceed the number of cells plated. B. Left panel: Primary Prdx1$^{-/-}$ and $^{+/+}$MEFs of different passages were stained for SA-βgal activity. Right panel: Quantification of B, (up to 4000 cells per passage and genotype were analyzed). C. Primary Prdx1$^{-/-}$ and $^{+/+}$MEFs were treated with increasing doses of H_2O_2 for 8 hours and analyzed by Western blotting for phosphorylation of p53 on Ser15 and p53 protein levels. D. Primary Prdx1$^{-/-}$ and $^{+/+}$MEFs were passaged in the absence and presence of 3μM and 6 μM of the p38MAPKα inhibitor SB203580, and

stained for SA-βgal activity at passages 3, 4, 5, and 6. Representative pictures showing senescent morphology and confluency were also taken. Quantification of cells positive for SA-βgal staining was performed; "*" denotes statistical significance. P-values for $Prdx1^{-/-}$ MEFs include: 0.027 (passage 3, 0μM SB203580 vs. 3μM); 0.007, 0.0036 (passage 4, 0μM SB203580 vs. 3μM, and 0μM SB203580 vs. 6μM, respectively); 0.000, 0.000 (passage 5, 0μM SB203580 vs. 3μM, and 0μM SB203580 vs. 6μM, respectively); and 0.022, 0.003 (passage 6, 0μM SB203580 vs. 3μM, and 0μM SB203580 vs. 6μM, respectively). For $Prdx1^{+/+}$MEFs: 0.007, 0.0036 (passage 4, 0μM SB203580 vs. 3μM, and 0μM SB203580 vs. 6μM, respectively), and 0.000, 0.0029 (passage 6, 0μM SB203580 vs. 3μM, and 0μM SB203580 vs. 6μM, respectively). E. $Prdx1^{-/-}$ and $^{+/+}$MEFs were plated on 10cm plates at 1.8×10^5 and serum-starved for 48 h in 0.25% FBS. Cells were treated with increasing amounts of H_2O_2 (25-200 μM) for 10min in serum-free medium. Following treatment, plates were washed with cold 1X PBS (pH 7.2-7.4) two times. Cell lysates were analyzed by SDS-PAGE and Western blotting for phosphorylation of p38MAPKα on Thr180 and Tyr 182, phosphorylation of the p38MAPKα substrate ATF2 on Thr 69 and 71, p38MAPKα protein levels, and actin as loading control. F. Quantification of three independent experiments analyzing phosphorylation of p38MAPKα and its substrate ATF2 as described under E. Density of Western blot bands were analyzed using Image J software (http://rsbweb.nih.gov/ij/). Densities of phosphorylated p38MAPKα and ATF-2 proteins bands were normalized to density of p38MAPKα protein bands. Values were normalized to density of untreated WT cells as 1. Three different sets of Prdx1 WT and KO clones were tested. "*" indicates statistical significance (Students T-test) of KO and matching WT clones treated with H_2O_2. P-values for phosphorylation of p38MAPKα were 0.038 (25μM H_2O_2), 0.039 (50 μM H_2O_2), 0.008 (100 μM H_2O_2) and 0.044 (200 μM H_2O_2). P-values for phosphorylation of ATF-2 were 0.022 (25μM H_2O_2), 0.037 (100 μM H_2O_2) and 0.044 (200 μM H_2O_2). G. $Prdx1^{-/-}$ and $^{+/+}$MEFs were plated as above and treated with increasing amounts of PDGF for 1-10 mins in phenol-free DMEM supplemented with 0.1% BSA. Following treatment, plates were washed with cold 1X PBS two times before lysing. Protein lysates were analyzed as above. H. Quantification of three independent experiments as described under F for protein lysates used in G. Four different sets of Prdx1 WT and KO clones were tested. "*" indicates statistical significance (students T-test) of KO and matching WT clone treated with PDGF. P-values for phosphorylation of p38MAPKα were 0.003 (0.5min), 0.004 (1min), 0.04 (5min), <0.0001 (7min) and 0.021 (10min). P-values for phosphorylation of ATF-2 were 0.015 (5min), 0.018 (7min) and 0.009 (10min).

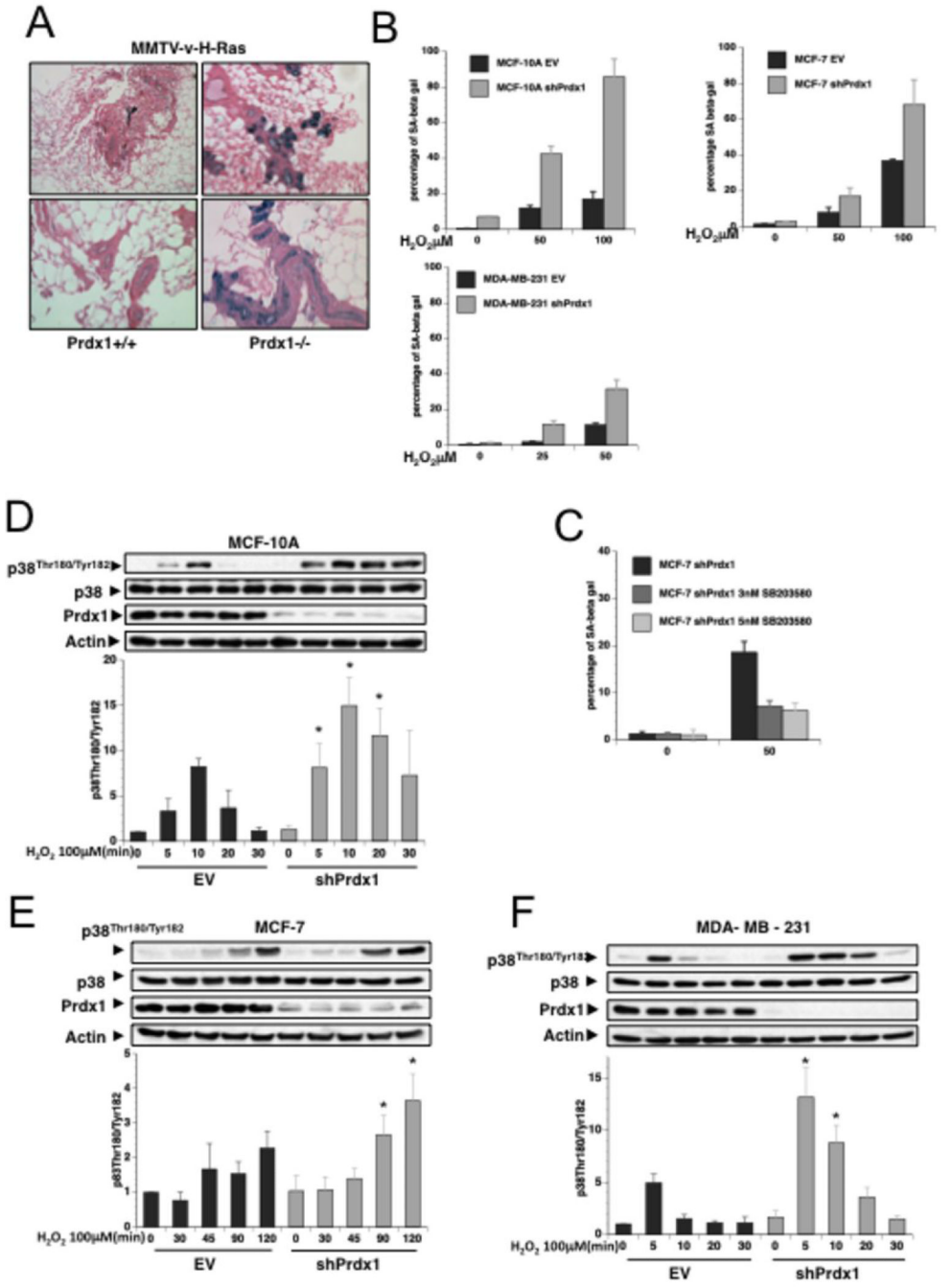

Figure 2. Prdx1 prevents ROS-induced senescence in breast epithelial cells

A. Mammary glands from 12-14 month old MMTV-H-Ras-Prdx1$^{+/+}$ and MMTV-H-Ras-Prdx1$^{-/-}$ were stained for SA-βgal activity. B. Prdx1 expression was decreased in various human breast epithelial cells using lentiviral shRNA. MCF-10A, MCF-7 and MDA-MB-231 cells expressing vector control (empty vector = EV) or shPrdx1 were plated at 35,000 cells/well in 6-well plates overnight. Cells were treated with H_2O_2 in DMEM containing 10% FBS for 4 days. Following treatment, cells were washed with sterile 1X PBS and incubated in fresh medium for 24 h, and sub-cultured at low confluency for 10 days. Plates were stained for SA-βgal activity as previously described (53). Up to 6000 cells per treatment and genotype were quantified. C. MCF-7 cells were plated overnight at 35,000 cells/well in 6-

well plates, and treated as in B with the addition of the p38MAPKα inhibitor SB203580 every two days before staining for SA-βgal activity. D-F. MCF-10A, MCF-7 and MDA-MB-231 cells expressing vector control (empty vector = EV) or shPrdx1 were plated in 6 cm dishes overnight at 8.0 X 10^4. The following day, medium was removed and the plates washed in 1X sterile PBS two times, and incubated in serum free medium for 120 minutes. Following equilibration in serum-free medium, cells were treated with 100 μM H_2O_2 for up to 2 h for MCF-7 cells, and 30 min for MCF-10A and MDAMB-231 cells. Cells were lysed with 150 μl of lysis buffer, and protein lysates were analyzed by Western blotting for p38MAPKα phosphorylation, p38MAPKα, Prdx1 knock down, and actin protein levels. Quantification of three to four independent experiments for each human breast epithelial cell line analyzing phosphorylation of p38MAPKα is placed below each cell line. Density of phosphorylated p38MAPKα Western blot bands were analyzed using Image J software (http://rsbweb.nih.gov/ij/) and normalized to densities of p38MAPKα protein bands. Lastly, values were normalized to density of untreated EV cells as 1. "*" indicates statistical significance (Students T-test) of shPrdx1 and matching EV clone treated with H_2O_2. P-values of p38MAPKα phosphorylation for MCF-10A: 0.049 (5min), 0.031 (10min) and 0.019 (20min); MBA-MD-231: 0.018 (5min) and 0.013 (10min); MCF-7: 0.011 (90min) and 0.028 (120min).

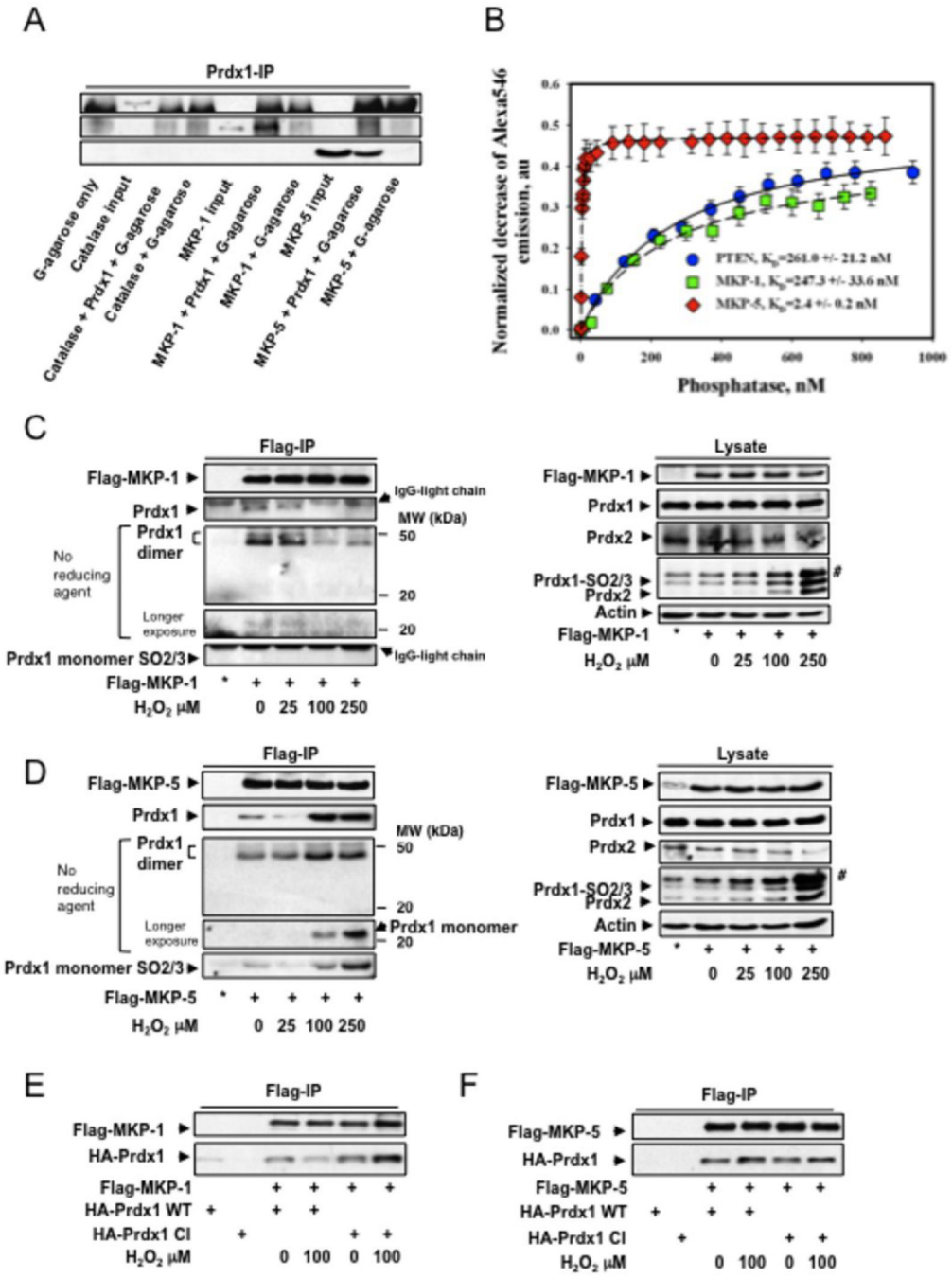

Figure 3. Non-covalent binding of Prdx1 to MKP-1 and MKP-5

A. Pull down of recombinant Catalase, MKP-1 and 5 by Prdx1 conjugated protein G agarose. The far left lane represents protein agarose G only to serve as a negative control for non-specific binding. B. Purified Prdx1 protein (2.0 nM) labeled with Alexa Fluor® 546 was titrated with indicated amount of the purified phosphatase proteins labeled with QSY® 35. Alexa546 fluorescence decrease (normalized to initial Alexa546 emission) was recorded and processed using a “One Site Saturation model” (Pharmacology application, SigmaPlot 10.0, SyStat, MA) with best hyperbolic fit ($R^2 \geq 0.99$) according to equation: $\mathbf{Y = B_{max} * X / (K_D + X)}$ where: X – is a concentration of added PTEN (MKP-1 or MKP-5) protein; Y – is

a normalized decrease of Alexa®546 fluorescence corresponding to specific binding of phosphatases; B_{max} – is a saturated number of binding sites with apparent equilibrium dissociation constant K_D. Data represent mean±SD for 3 independent experiments. The lines represent hyperbolic fit of experimental data for the titration of 2.0 nM of Alexa546-labeled Prx1 with QSY35-labeled: PTEN – solid line (R^2=0.99); MKP-1 - dashed line (R^2=0.99); and MKP-5 - doted and dashed line (R^2=0.99). C and D. 293T HEK cells were transfected with 2.0μg of Flag-MKP-1 and Flag-MKP-5, and treated with increasing amounts of H_2O_2 for 30 min in serum free medium. To assay for binding of endogenous Prdx1, 1000 μg of protein lysate was immunoprecipitated using anti-flag affinity matrix and incubated 3 hrs at 4^0C in an hypoxic chamber. The affinity matrix was harvested by centrifugation at 3000xg for 2 min, and washed with 0.5 ml of lysis buffer 3 times. The resin was re-suspended in 20 μl of reducing or non-reducing SDS-PAGE sample buffer, boiled 10 mins, and analyzed by Western blotting for MKP expression, Prdx1 and Prdx1Cys52SO3 binding. * = IP from untransfected cells. Co-IPs were also analyzed in the absence of β-mercaptoethanol. No Prdx1 dimer staining positive for SO2/3 were detected. #: detection of a higher molecular weight 2-Cys Prdx family member. Co-IP unbound fraction can be found in the supplemental material Fig. S3B. E and F. 293T HEK cells were cotransfected with Flag-MKP-1 or Flag-MKP-5 either with HA-Prdx1WT or HA-Prdx1CI, and treated with increasing amounts of H_20_2 for 30 min in serum free medium. For co-IP, 1000μg of lysate was added to anti-flag affinity matrix and incubated for 1h at 4^0C. Following incubation, the affinity matrix was harvested as stated above, re-suspended in 20μl of reducing sample buffer, and boiled for 10 min. Binding of HA-Prdx1WT and HA-Prdx1CI was determined by Western blotting. Analysis of cell lysate for protein expression can be found in the supplemental material Fig. S3C.

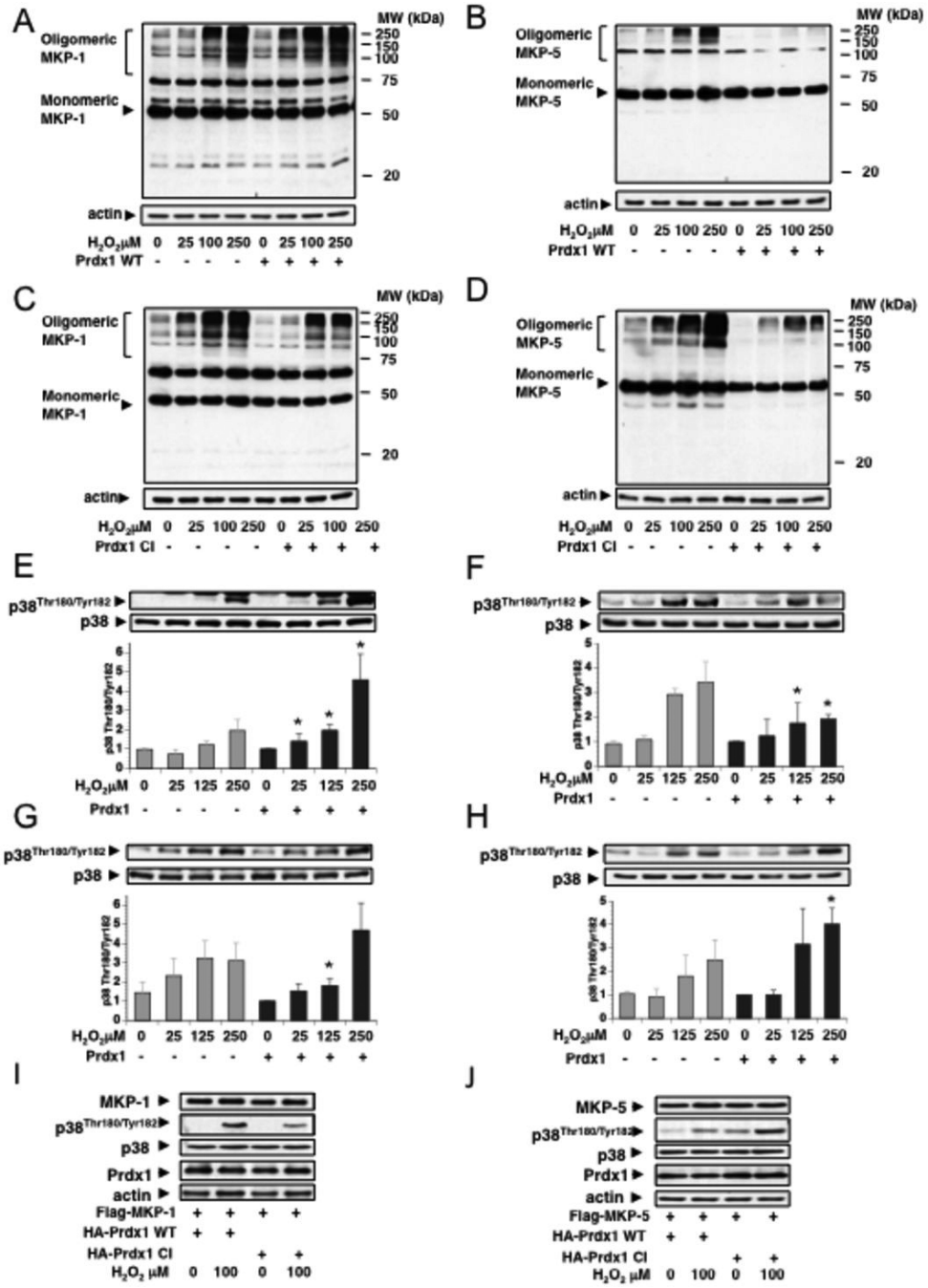

Figure 4. Prdx1 protects MKP-5 from oxidation-induced oligomerization and inactivation

A and B. Flag-MKP-1 or Myc-MKP-5 were overexpressed together with untagged Prdx1 in 293T cells, using 1.0 μg of DNA. (Note: initial experiments included N-terminal tagged Prdx1 proteins. This enhanced slightly the MKP-1 oligomerization; we therefore used untagged Prdx1). Cells were treated for 30 min with increasing concentrations of H_2O_2 in serum-free medium, and protein lysates analyzed under non-reducing conditions by Western blotting for oligomerization of MKP-1 and MKP-5 (n= 3). C and D. As in A and B, with the exception of co-expressing untagged Prdx1-CI. (n=3) E-H, Western blot analysis of A-D for phosphorylation of p38MAPKα. Quantification include three independent experiments. Density of phosphorylated p38MAPKα Western blot bands were analyzed using Image J

software (http://rsbweb.nih.gov/ij/) and normalized to densities of p38MAPKα protein bands. Lastly, values were normalized to density of untreated cells expressing exogenous Prdx1. P-values of p38MAPKα-phosphorylation for MKP-1 + WT-Prdx1: 0.011 (25μM H_2O_2), 0.002 (100μM H_2O_2), 0.004 (250μM H_2O_2). MKP-1 + CI-Prdx1: 0.01 (100μM H_2O_2). MKP-5 + WT-Prdx1: 0.04 (100μM H_2O_2), 0.013 (250μM H_2O_2). MKP-5 + CI-Prdx1: 0.014 (250μM H_2O_2). Western blots showing MKP-1 or MKP-5 co-expressed with Prdx1 WT or Prdx1 CI run under non-reducing conditions can be found in the supplemental information along with Western blot analysis under reducing conditions (Figs. 4SA and 4SB). I and J. 293T HEK cells were co-transfected with Flag-MKP-1 or Flag-MKP5 and with Prdx1 WT or Prdx1 CI, respectively, and treated with increasing amounts of H_2O_2 for 30 min in serum free medium. Lysates were run under reducing conditions, and analyzed by Western blotting for phosphorylation of p38MAPKα on Thr180 and Tyr182, expression of p38MAPKα, MKPs and Prdx1.

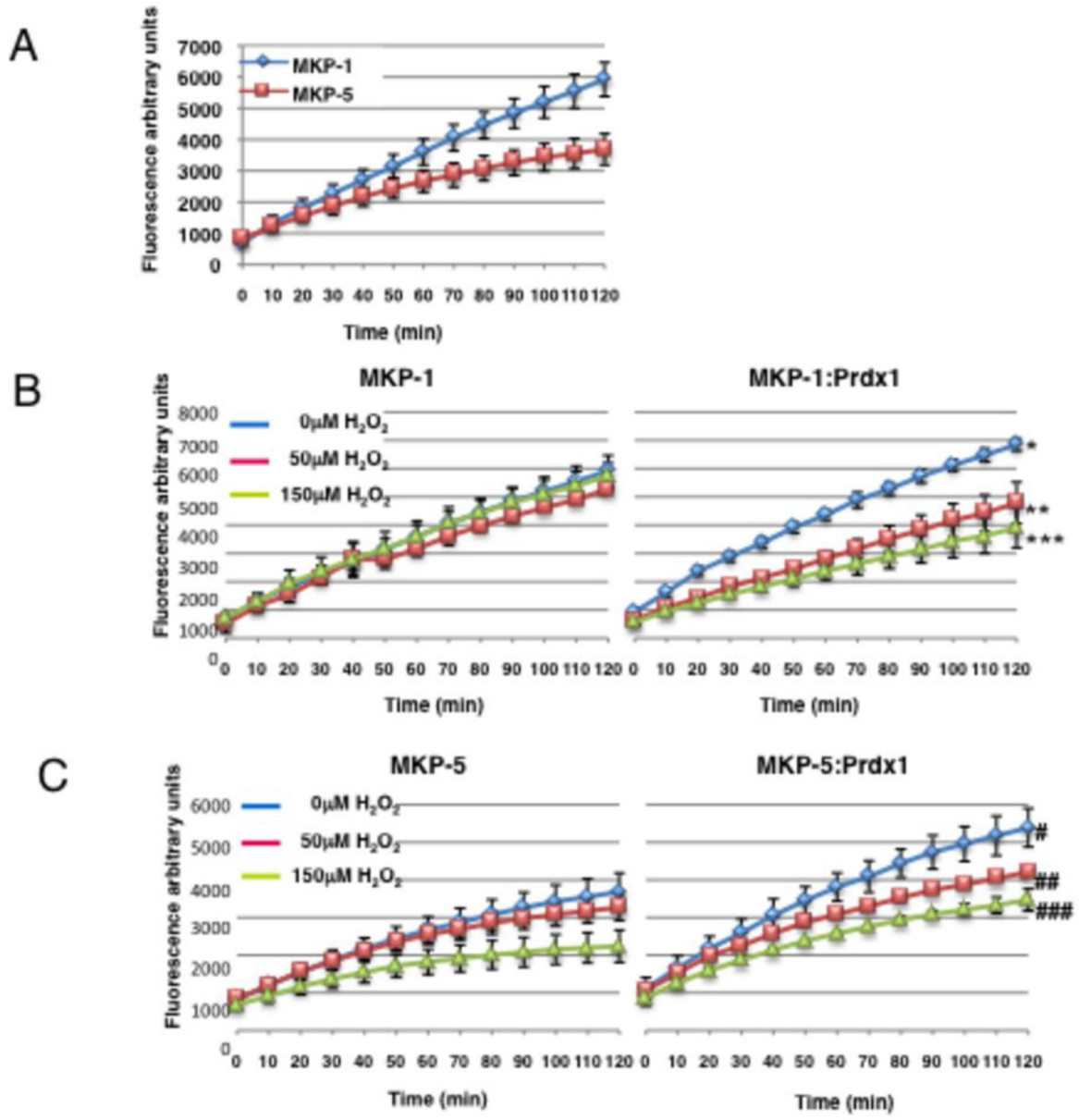

Figure 5. Prdx1 promotes MKP-5 catalytic activity and protects it from H_2O_2-induced stress

Time courses of 160 μM DiFMUP hydrolysis by recombinant MKP-1 and MKP-5 phosphatase activity was measured in the presence of Prdx1 and H_2O_2. An equimolar ratio of MKP:Prdx1 recombinant protein was added to 1X reaction buffer in 1.5ml eppendorf tubes at room temperature. Concentrations of MKPs were kept the same in each reaction. H_2O_2 was diluted in sterile H_2O, and added to the recombinant proteins and allowed to incubate at room temperature for 10 min. The proteins were pipetted into a black, clear bottom 96 well plate, followed by the addition of 160 μM of DiFMUP substrate. The plate was covered in foil, and read at ~360/460nm on a fluorescence plate reader every 10 min for 2 h. X-axis represent time in minutes, y-axis represent flourescent signal generated DiFMUP hydrolysis. A. Comparison of MKP-1 and MKP-5 catalytic activity. B. Left panel: MKP-1 activity over time in the presence of increasing concentrations of H_2O_2. Right panel: same as in left panel in the presence of Prdx1. C. Left panel: MKP-5 activity over time in the presence of increasing concentrations of H_2O_2. Right panel: same as left panel, in the

presence of Prdx1. Statistical analysis: Utilization of substrate was measured for MKP-1 and MKP-5 at three levels of H_2O_2 concentration (0, 0.05, 0.15 mM) in the absence or presence of Prdx1. Prdx1 treatment effects over time on MKP activity were modeled in a random effects model, allowing for fixed effects of Prdx1, time in minutes. Random intercepts and experimental effects were included. The six tests of differences in treatment effects (MKP activity without Prdx1 compared to MKP activity in the presence of Prdx1) over time were all statistically significant at the $\alpha = 0.05$ level. *: p<0001, **: p=0.0121, ***: p<0.0001; #: p<0.0001, ##: p<0.0001, ###: p<0.0001. Moreover, differences in H_2O_2 concentration effects over time were also tested within Prdx1 treated samples: for MKP1, H_2O_2 differences over time: $p < 0.0001$; for MKP5, H_2O_2 differences over time: $p = 0.0002$.

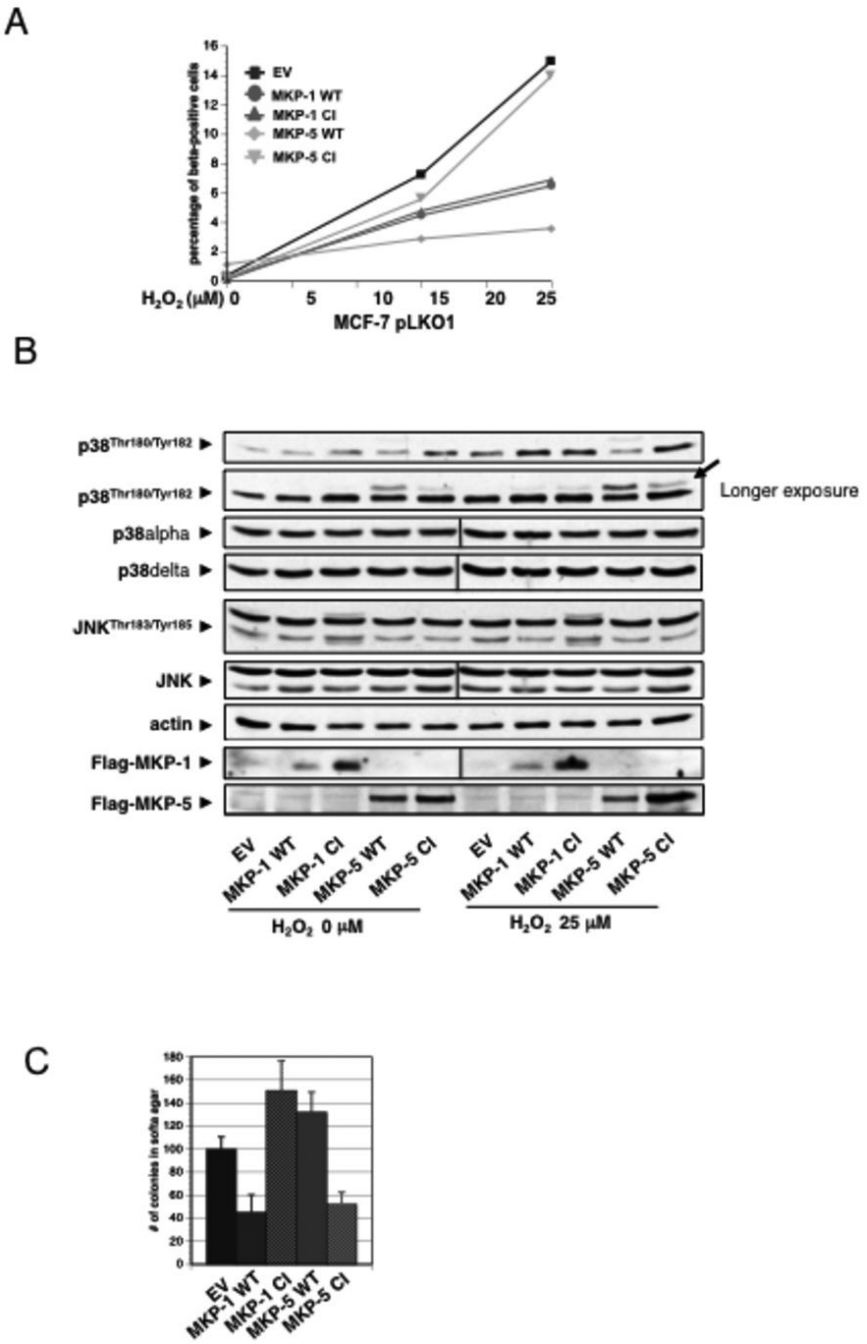

Figure 6. Prdx1 prevents ROS-induced senescence in MCF-7 cells by promoting MKP-5 activity

A and B. MCF-7 cells were infected with retrovirus for Flag tagged MKP-1 WT, MKP-1 C258S, MKP-5 WT or MKP-5 C408S and 7 days later with lentivirus for shPrdx1 or EV. After 5 days of selection, cells were plated overnight at 35,000 cells/well in 6 well plates and treated with H_2O_2 every day for 4 days in DMEM containing 10% FBS. Following treatment, cells were allowed to recover for 10 days in fresh medium, and stained for SA-β-gal activity as previously stated. Blue cells were quantified as described in Fig. 2. Plot is a representative of two independent experiments. MCF-7 cells expressing MKP-1 and MKP-5 WT and CI mutants were plated in 6 cm dishes overnight at 8.0 X 10^4, and then treated with 5μM of MG132 proteasome inhibitor overnight. The following day, medium was removed

and the plates washed in 1X sterile PBS two times, and incubated in serum free medium for 120 minutes. Following equilibration in serum-free medium, cells were treated with 25 μM H_2O_2 treatment for 2 h. Cells were lysed with 150 μl of lysis buffer, and protein lysates were analyzed by Western blotting for p38MAPKα phosphorylation on Thr180/Tyr182, JNK phosphorylation on Thr183/Tyr185, p38MAPKδ levels, and actin protein levels. Arrow indicates slower migrating band, which could be phosphorylated p38MAPKδ. C. Cells from A were plated in soft agar, and colonies were counted.

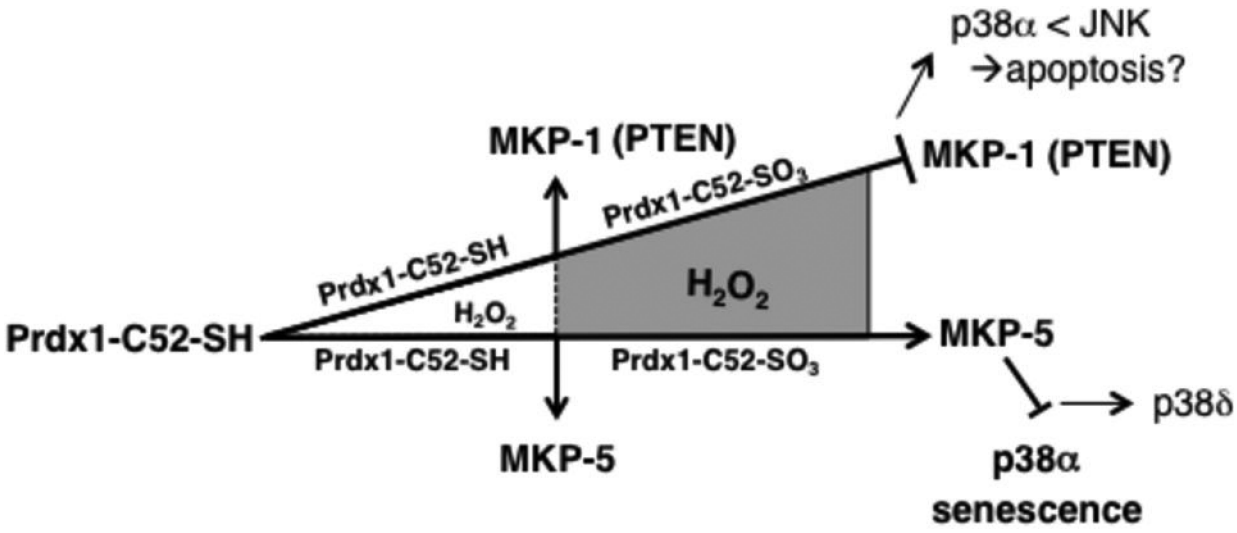

Figure 7. The peroxidatic cysteine Cys52 of Prdx1 is a sensor in ROS-signaling

Under normal ROS homeostasis, Prdx1 promotes both MKP-1 and MKP-5 activity. However, under increased ROS, Prdx1-Cys52-SO3 forms less Prdx1/MKP-1 complexes leading to MKP-1 inactivation. This is comparable to data we obtained for PTEN(7). Conversely, in the presence of MKP-5, Prdx1-Cys52-SO3 binds to MKP-5 and preserves MKP-5 activity. We therefore speculate that MKP-1, which in some instances prefers JNK over p38MAPKα as a substrate (52) is inactivated under high oxidative stress (because of the dissociation from Prdx1) to allow JNK activity. MKP-5 on the other hand favors, depending on the cellular context, p38MAPKα over JNK as a substrate (53). This way, MKP-5 activation by Prdx1 is thereby preventing p38MAPKα signaling in H_2O_2-induced senescence. The net outcome of all this may be that Prdx1 in a H_2O_2-dose dependent manner prevents oxidative p38MAPKαmediated stress-induced senescence to promote JNK mediated signaling.

Table 1

Lack of Prdx1 in MMTV-v-H-Ras mice increases SA-β-gal activity in mammary glandular structures

Mammary glands from MMTV-v-H-Ras Prdx1$^{+/+}$ or Prdx1$^{-/-}$ were collected and small pieces (.5 × .5cm) were processed for SA-β-gal activity.

SA-β-gal activity (staining intensity)	Ø	+	++	+++
MMTV-v-H-Ras Prdx1 +/+	3	3	1	0
MMTV-v-H-Ras Prdxl −/−	0	2	2	3

Table 2
Non-covalent binding of Prdx1 with MKP-5, MKP-1 and PTEN

To address if covalent binding exists between Prdx1 and MKP-1 or MKP-5, the reducing agent TCEP was added to the FRET-based fluorescent analysis shown in Fig. 3SA. This resulted in comparable K_Ds for MKP-5 and for MKP-1

K_D	−TCEP	+TCEP
MKP-5	2.5±0.4 nM	3.1±0.5 nM
MKP-1	210±19.5 nM	215.0±21.5 nM
PTEN	215.0±19.5 nM	219.5±22.5 nM